44th AIAA Aerospace Sciences Meeting and Exhibit
9 - 12 January 2006, Reno, Nevada

AIAA 2006-1471

Multi-objective Aerodynamic Optimization of Elements' Setting for High-lift Airfoil Using Kriging Model

Mashiro Kanazaki*
Japan Aerospace Exploration Agency (JAXA), Chofu, Tokyo, 182-8522, Japan

Kentaro Tanaka†
Ryoyu systems Co., Ltd., Minato-ku, Tokyo, 108-0074, Japan

Sinkyu Jeong‡
Tohoku University, Aoba-ku, Sendai,980-8577 ,Japan

and

Kazuomi Yamamoto§
Japan Aerospace Exploration Agency (JAXA), Chofu, Tokyo, 182-8522, Japan

In this paper, a multi-objective design optimization for a three-element airfoil consisted of a slat, a main wing, and a flap was carried out. The objective functions were defined as the maximization of lift coefficient at landing (C_{l8}) and near stall (C_{l20})conditions simultaneously. Genetic Algorithm (GA) was used as an optimizer. Although it has advantage of global exploration, its computational cost is expensive. To reduce the computational cost, the kriging model which was constructed based on several sample designs was introduced. The solution space was explored based on the maximization of Expected Improvement (EI) value corresponding to objective functions on the kriging model to consider the predicted value by kriging model and its uncertainty. The improvement of the model and the exploration of the optimum can be advanced at the same time by maximizing EI value. In this study, 90 sample points are evaluated using the Reynolds averaged Navier-Stokes simulation (RANS) for the construction of the kriging model. Through the present exploration process, several designs were obtained with better performance than the baseline setting in each objective function. Functional Analysis of Variance (ANOVA) which is one of the data mining techniques showing the effect of each design variable on the objectives is applied. Main-effects of the design variables are calculated to recognize which design variable has the effect on the objective functions. This result suggests that the gap and the deflection of the flap have a remarkable effect on each objective function and the gap of the slat has an effect on C_{l20}.

* Researcher, Civil Transport Team, Aviation Program Group, 7-44-1 Jindaiji-Higashi, Chofu, Tokyo, 182-8522, JAPAN, AIAA Member
† Engneer, Engineering Solution Division, 2-19-13, Takanawa, Minato-ku, Tokyo, 108-0074, JAPAN
‡ Assistant, Institute of Fluid Science, 2-1-1 Katahira Aoba-ku, Sendai, 980-8577, JAPAN, Associate Member AIAA
§ Senior Researcher, Civil Transport Team, Aviation Program Group, 7-44-1 Jindaiji-Higashi, Chofu, Tokyo, 182-8522, JAPAN, AIAA Member

Nomenclature

C_l	=	lift coefficient
c	=	chord length of airfoil when flap and slat are retracted into the main element
$overlap_{slat}$	=	slat overlap between slat and main wing
gap_{slat}	=	slat gap between slat and main wing
θ_{slat}	=	deflection angle of slat
$overlap_{flap}$	=	flap overlap between flap and main wing
gap_{flap}	=	flap gap between slat and main wing
θ_{flap}	=	deflection angle of flap
α	=	angle of attack
$C_{l\alpha}$	=	lift coefficient at the angle of attack of α degree
$y(\cdot)$	=	unknown function
x	=	scalar component of $\boldsymbol{x}$
$\boldsymbol{x}$	=	vector denoting position in the design space
μ	=	constant global model of kriging model
$\varepsilon(\cdot)$	=	deviation from constant model
$E[I(\cdot)]$	=	expected improvement
$\hat{y}$	=	predicted value on the model
$f_{\max}$	=	maximum value among sample points
s^2	=	mean squared error of the predictor
Φ	=	standard normal distribution
ϕ	=	standard normal density
$EI_{Cl\alpha}$	=	EI value for $C_{l\alpha}$
C_p	=	pressure coefficient

I. Introduction

A civil aircraft wing is generally designed by considering about a cruise condition. On the contrary, when an aircraft lands or takes off, its wing should gain enough lift even at low-speed. In such condition, high-lift system which can increase the wing load at low-speed is required. Thus, high-lift system is one of the main interests in aircraft design due to its effect on landing/ take-off performances, and pay-load capacity of an aircraft.

One of a typical high-lift system is a multi-element wing. Flowfield around a multi-element wing has a complex physics caused by the interaction of each element.[1, 2] One of the important physics is *circulation effect*. The circulation of a forward element reduces the leading edge suction peak of a trailing element, thus delaying separation. Moreover, the trailing element induces a circulation effect on the forward element and increases the loading on the element. Additionally, viscous effect of wakes from each element is existent. It provides a damping effect on the pressure peak of trailing element. However, wakes often merge with the boundary layer of the trailing element and boundary layer becomes much thinner, as a result, the separation increases. Thus, the high-lift system should be designed with considering complex flow physics described above. To evaluate such physics, the high-fidelity evaluation of a high-lift system is desirable in a design process.

Recently, many studies to develop the high-fidelity flow solver using Navier-Stokes simulation around a high-lift system have been carried out and they are validated. [3-5] Thus, the relevant design considering accurate flow physics can be expected. To introduce high-fidelity evaluation, it is required to employ high efficient design procedure to reduce the computational cost. There are several efforts about the high-fidelity optimization with considering design efficiency. [6, 7] In Ref. 6, Navier-Stokes design of a high-lift system based on finite difference sensitivity evaluation with a few design iterations. In Ref. 7, kriging model was introduced and perform the global optimization and reduce the total computational cases.

In this study, kriging surrogate model and MOGA (multi-objective GA) is applied to multi-objective design problem. The three-element airfoil as shown in Fig. 1 is used as a baseline setting. Generally, a slat increases the stall angle and a flap produces an upward shift in a lift curve as shown in Fig. 2 [1], thus multi-angle of attack should

be considered. In this study, the multi-objective design of the three-element high lift system is defined, where objective functions are to maximize C_l at the angle of attack of 8 degree which corresponds to landing condition and 20 degree which corresponds to near stall angle and the design variables are element' settings.

Kriging model allows efficient searching process, resulting in drastic reduction in computational time. In this study, two kriging model corresponding to each objective functions are constructed. EI (Expected Improvement) value [7, 8] calculated on the model is used as a criterion to select additional sample points after initial sampling constructs kriging models. They make it possible not only to improve the accuracy of the kriging model but also to explore the global optimum efficiently. EI values are maximized using DRMOGA (Divided Range MOGA) [9, 10] which is one of the modified versions of MOGA.

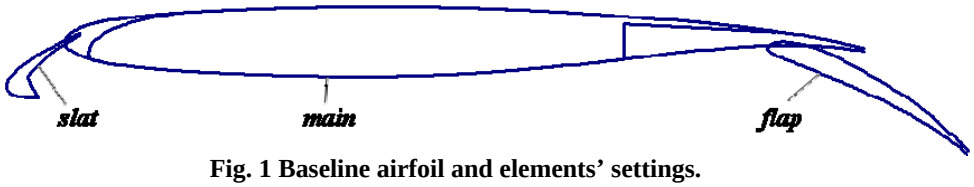

Fig. 1 Baseline airfoil and elements' settings.

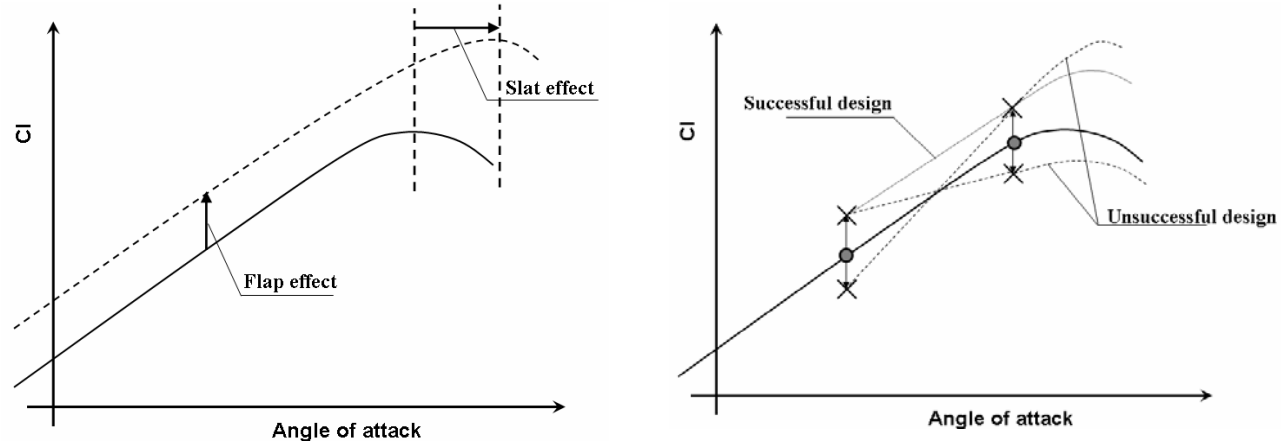

Fig. 2 High-lift system effect on airfoil lift and ideal design.

II. Formulation

A. Flow Solver

Aerodynamic performances of sample designs for kriging models are evaluated using a structured multi-block flow solver, UPACS (Unified Platform for Aerospace Computational Simulation) [12]. UPACS is developed at JAXA as a common-base code for aerodynamic researchers.

In this study, RANS is applied with Spalart-Allmaras turbulence model. Flux was evaluated by Roe's flux difference splitting with MUSCL for third-order spatial accuracy. The computational grid as shown in Fig. 3 is decomposed into 35 sub-domains. Number of cells is about 10,000. To reduce mesh generation time, the deforming mesh method [13] is applied to deform the mesh around the baseline setting. Mach number is set to 0.2 and Reynolds number is set to 1.24×10^7. As the first step of multi-objective optimization using the kriging model, we do not intend to include transition in the calculations which should affect lift characteristics of high-lift system. Thus, the boundary-layer is treated fully turbulent.

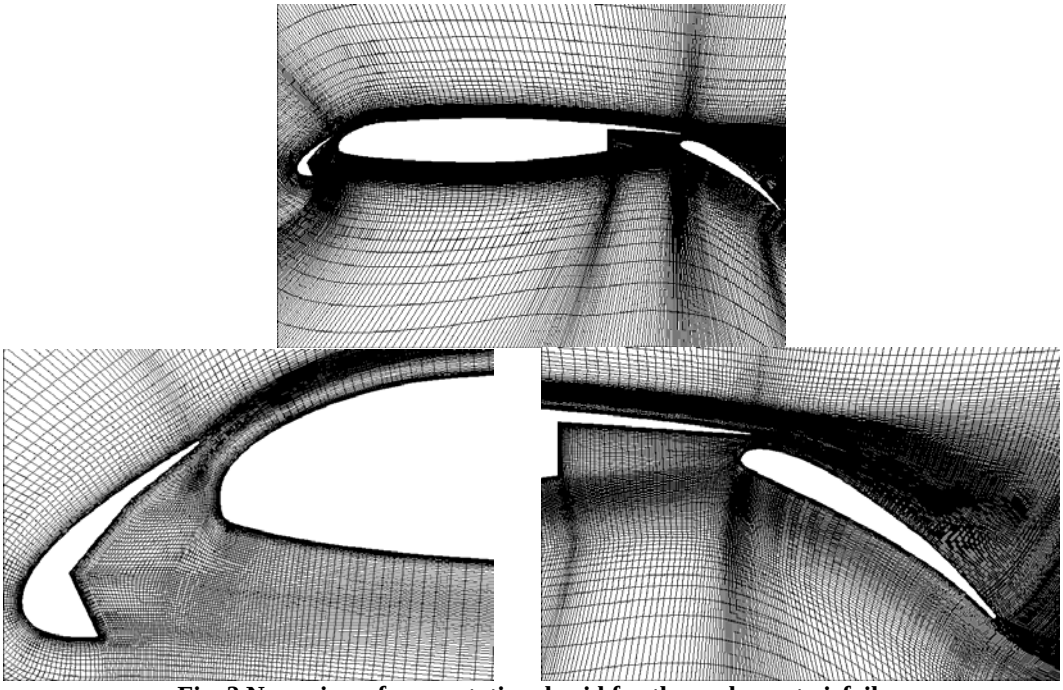

Fig. 3 Near view of computational grid for three-element airfoil.

B. Design Variables

As shown in Fig. 4, the overlap, the gap, and the deflection angle between elements are used as the design variables. Each design variable in limited as follows:

$$-0.01\ c \le overlap_{\text{slat}} \le 0.01\ c$$
$$0.01\ c \le gap_{\text{slat}} \le 0.04\ c$$
$$20.0 \le \theta_{\text{slat}} \le 30.0 \text{ (degree)}$$
$$-0.01\ c \le overlap_{\text{flap}} \le 0.01\ c$$
$$0.01\ c \le gap_{\text{flap}} \le 0.03\ c$$
$$30.0 \le \theta_{\text{flap}} \le 40.0 \text{ (degree)}$$

where c is the chord length of airfoil when flap and slat are retracted into the main element.

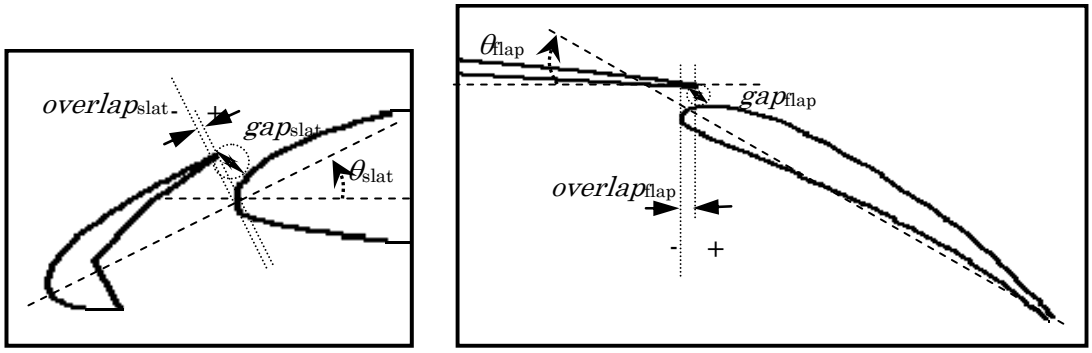

Fig. 4 Design parameters.

C. Objective functions

In this study, the design problem has two objective functions. The objective functions considered here are to maximize lift co-efficients at angle of attack of 8 degree (C_{l8}) and 20 degree (C_{l20}). Angle of attack of 8 degree is assumed the angle of attack at landing condition and 20 degree is assumed the stall angle decided from C_l-α of the baseline setting as discussed in the following paragraph.

The baseline setting was calculated for several angles of attack. The baseline settings (Fig. 1) are as follows:

$overlap_{slat}$: 0.005 c
gap_{slat}: 0.01687 c
θ_{slat}: 25 (degree)
$overlap_{flap}$: 0.01 c
gap_{flap}: 0.0166 c
θ_{flap}: 35 (degree)

Figure5 shows lift curve for baseline configuration obtained by RANS. From this result, this airfoil stalled at angle of attack of 20-22 degree. From this result, the angle of attack of 20 degree was decided as the near stall design condition.

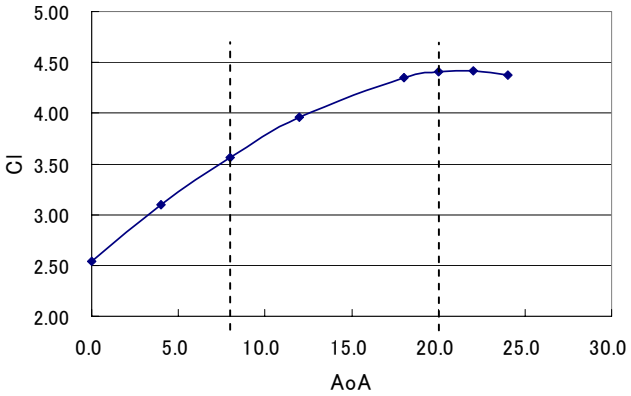

Fig 5 Lift co-efficient for Baseline configuration.

D. Multi-objective Design Exploration Based on Kriging model

The procedure of the present design (Fig. 6) is as follows: First, N samples which are decided by Latin hypercube sampling [14] which is one of the space filling methods are evaluated using RANS and kriging surrogate models are constructed. Then, m EI maximum points are added as sample points, and model accuracy is improved by constructing kriging models using $N+m$ samples. This process is iterated until improvement of objective functions becomes little. Finally, data mining technique can be applied to obtain the information of the design problem. The detail of each procedure is described in the following sections.

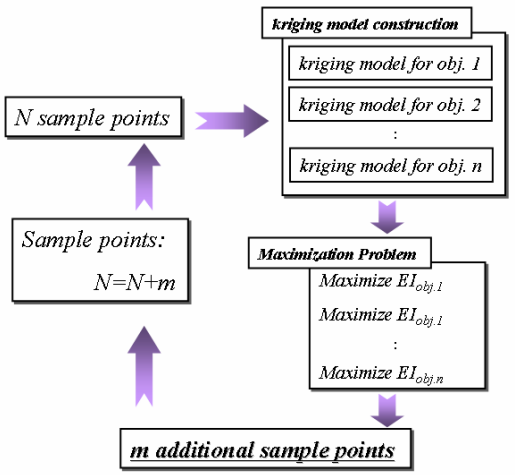

Fig.6 Procedure of multi-objective global exploration.

1. kriging model

Kriging model [7] expresses the value $y(x^i)$ at the unknown design point x^i as:

$$y(x^i) = \mu + \varepsilon(x^i) \quad (i = 1, 2, \ldots, m) \qquad (1)$$

where, m is the number of design variables, μ is a constant global model and $\varepsilon(x^i)$ represents a local deviation from the global model. In the model, the local deviation at an unknown point $\boldsymbol{x}$ is expressed using stochastic processes. Some design points are calculated as sample points and interpolated with Gaussian random function as the correlation function to estimate the trend of the stochastic process.

2. Improvement of kriging model and selection of additional samples

Once the models are constructed, the optimum point can be explored using an arbitrary optimizer on the model. However, it is possible to miss the global optimum, because the surrogate model includes uncertainty at the predicted point. This study introduced EI values [7, 8] as the criterion.

EI for present maximization problem can be calculated as follows:

$$E[I(\mathbf{x})] = (\hat{y} - f_{\max})\Phi\left(\frac{\hat{y} - f_{\max}}{s}\right) + s\phi\left(\frac{\hat{y} - f_{\max}}{s}\right) \qquad (2)$$

where $f_{\max}$ is the maximum value among sample points and $\hat{y}$ is the value predicted by Eq. (1) at an unknown point $\boldsymbol{x}$. Φ and ϕ are the standard distribution and normal density, respectively. By selecting the point where EI takes the maximum value, as the additional sample point, robust

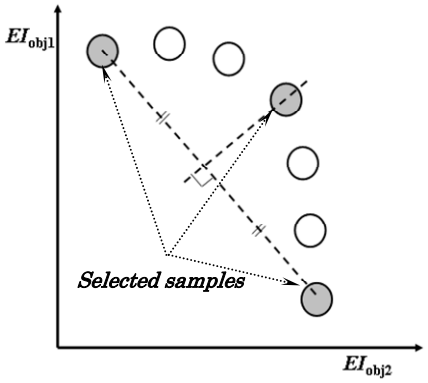

Fig. 7 Selection of additional samples based on EI maximization.

exploration of the global optimum and improvement of the model can be achieved simultaneously because this point has a somewhat large probability to become the global optimum. To apply multi-objective problem, this study considers two EI values based on two kriging models; EI_{Cl8} and EI_{Cl20}. Eq. (2) can be written for the present design problem as follows:

$$\begin{aligned} &\textit{maximize}: \quad EI_{Cl8} = (\hat{y} - C_{l8\_\max})\Phi\left(\frac{\hat{y} - C_{l8\_\max}}{s}\right) + s\phi\left(\frac{\hat{y} - C_{l8\_\max}}{s}\right) \\ &\textit{maximize}: \quad EI_{Cl20} = (\hat{y} - C_{l20\_\max})\Phi\left(\frac{\hat{y} - C_{l20\_\max}}{s}\right) + s\phi\left(\frac{\hat{y} - C_{l20\_\max}}{s}\right) \end{aligned} \tag{3}$$

Maximizing these objective functions, non-dominated solutions between EI_{Cl8} and EI_{Cl20} can be obtained. Among these non-dominated solutions, three points are selected as additional sample points (Fig. 7): i) the point whose EI values of C_{l8} is maximum, ii) the mid point in the non-dominated solutions and iii) the point whose EI values of C_{l20} is maximum. Therefore, the value of m becomes 3 in this study.

3. DRMOGA

DRMOGA procedure shown in Fig. 7 can be explained as follows [9, 10]. First, initial individuals are produced randomly and evaluated. Second, the division of individuals is performed by using the rank of individuals based on values of a certain objective function f_i. Assuming n subpopulations for N individuals, N/n individuals will be allocated to each subpopulation. Then in each subpopulation, the existing MOGA [9] is performed. After MOGA is performed for k generations, all of the individuals are gathered and they are divided into subpopulations again according to the ranking based on another objective function f_j. This ranking function will be chosen in turn. For present DRMOGA, k was set to 4 and a number of subpopulation n was set to 4.

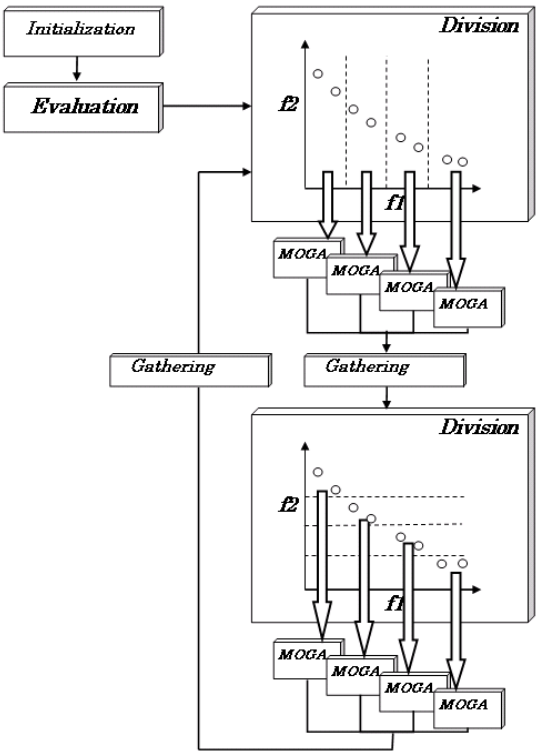

Fig. 7 Procedure of Distributed MOGA.

4. Data mining technique: ANOVA

An ANOVA [11] which is one of the data mining techniques is carried out to differentiate the contributions to the variance of the response from the model.

To evaluate the effect of each design variable, the total variance of the model is decomposed into that of each design variable and their interactions. The decomposition is accomplished by integrating variables out of the model $\hat{y}$. The main effect of design variable x_i is as follows:

$$\mu_i(x_i) \equiv \int \cdots \int \hat{y}(x_1, ..., x_n) dx_1, ..., dx_{i-1}, dx_{i+1}, .., dx_n - \mu \tag{4}$$

Two-way interaction effect x_i and x_j is written as:

$$\mu_{i,j}(x_{i,j}) \equiv \int \cdots \int \hat{y}(x_1, ..., x_n) dx_1, ..., dx_{i-1}, dx_{i+1} ..., dx_{j-1}, dx_{j+1}, .., dx_n - \mu_i(x_i) - \mu_j(x_j) - \mu \tag{5}$$

where, total mean μ is as follows:

$$\mu \equiv \int \cdots \int \hat{y}(x_1, ..., x_n) dx_1, ..., dx_n \tag{6}$$

The variance due to the design variable x_i is

$$\varepsilon \equiv \int \left[\mu_i(x_i)\right]^2 dx_i \tag{7}$$

The proportion of the variance due to design variable x_i to total variance of model can be expressed as:

$$p \equiv \frac{\varepsilon}{\int \cdots \int [\hat{y}(x_1,....,x_n) - \mu]^2 dx_1 \ldots dx_n} \tag{8}$$

The denominator of Eq. (8) means variance of the model. The value obtained by Eq. (8) indicates the sensitivity of the objective function to the variation of the design variable.

III. Results

A. Kriging Model

First, to construct the initial kriging model, 30 sample designs were evaluated by UPACS. Then, to explore better solutions based on EI maximization, the samples were added 20 times, as a result, 60 samples were added.

Fig. 8 (a) and (b) show C_{l8} plots against θ_{flap}-gap_{flap} predicted by kriging model obtained from initial 30 sample designs and additional samples (a total of 90 samples), respectively. According to Fig. 8, smaller gap between a flap and a main wing produces higher C_{l8}. Besides, Fig. 8 (b) shows larger deflection of flap (around 39 degree) produces higher C_{l8} than Fig. 8 (a). Moreover, the maximum of C_{l8} became sharpen, therefore, the design range which shows better aerodynamic performance emerged. This result shows that the present method find the optimum by the additional sampling.

Fig. 9 (a) and (b) show C_{l20} plots against θ_{slat}-gap_{slat} predicted by kriging model obtained from initial 30 sample designs and additional samplings, respectively. According to Fig. 9, the design point achieving maximum C_{l20} moved. This result suggests that the model was improved correctly, because the maximum of C_{l20} also became sharpen.

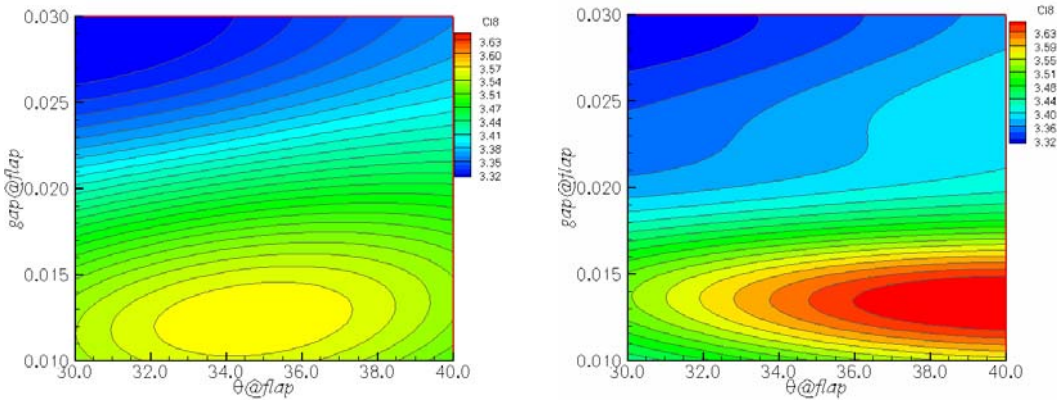

(a) (b)

Fig. 8 C_{l8} plots predicted by the kriging model about θ_{flap}-gap_{flap}: (a)from initial samples, (b)from additional samples.

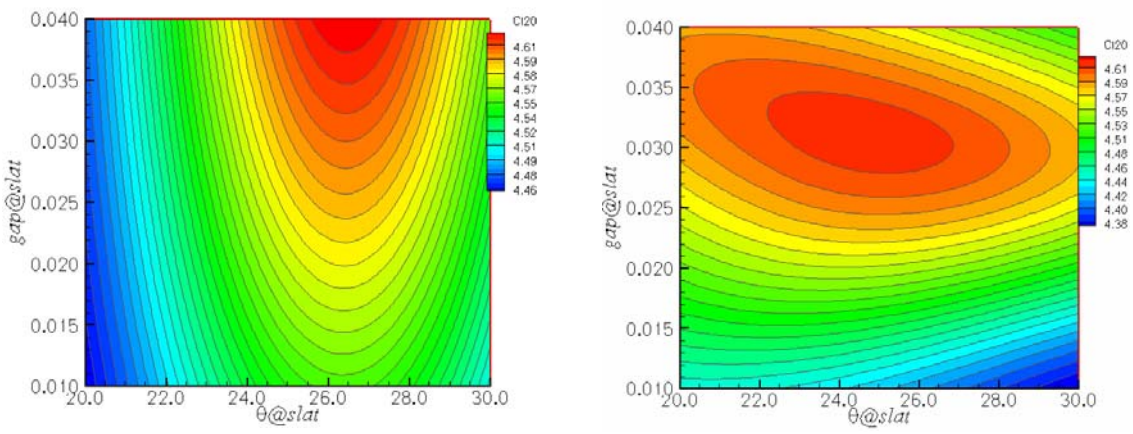

(a) (b)

Fig. 9 C_{l20} plots predicted by the kriging model about θ_{slat}-gap_{slat}: (a)from initial samples, (b)from additional samples.

B. Comparison of Solutions Chosen from Sampling result

Figure10 shows the solutions obtained based on the present method. From this figure, the solutions obtained from the initial sampling distributed uniformly in the solution space, on the other hand, the solutions obtained from 15th-20th additional samplings achieve the better performance than that of the initial samplings. The non-dominated front gradually advances to the optimum direction as the improving process is proceeded.. These results show that the present method selects the additional samples properly.

The elements' settings obtained from additional samplings (Design1, 2 and 3 shown in Fig. 10) are compared. Figure11 illustrated the comparison of their settings with the baseline setting. Every selected design dominates the baseline setting in the solution space. Thus, these settings have similar characteristics; Gap of slat and deflection angle of flap becomes larger.

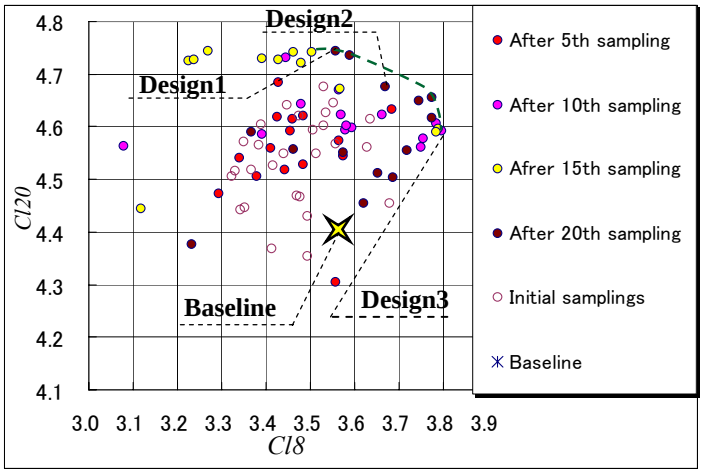

Fig. 10 Sample points obtained based on EI maximization.

C_p distributions of the baseline and the selected designs are compared as shown in Figs. 12, 13 and 14. According to Fig. 12 (b), the suction peak at the leading edges of the mother element and the flap of the design1 are higher than that of the baseline, thus, design1 achieves highest C_{l20}. According to Fig. 13(a), the C_p value on the upper surface of the mother element of the design2 is lower than that of the design1. As a result, C_{l8} of the design2 is higher than that of design1. Figure 14(a) shows that C_p value on the upper surface of the mother element of the design3 is entirely lower than that of the baseline. Consequently, design3 achieves the highest C_{l8}.

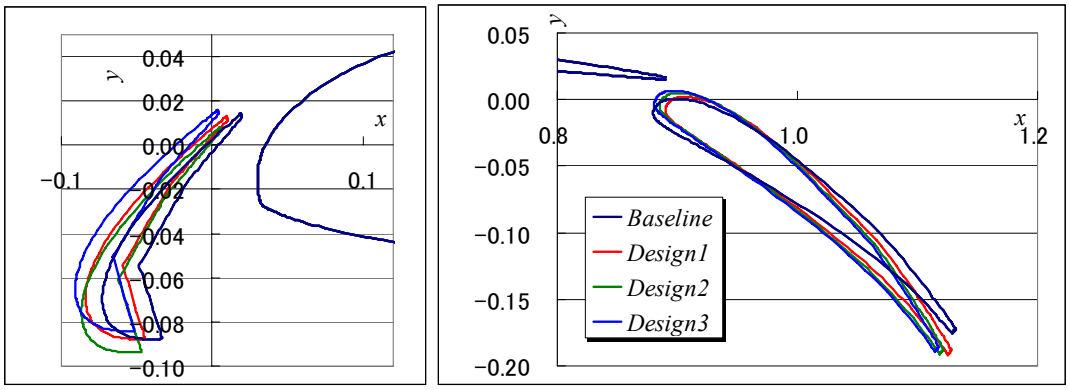

Fig. 11 Comparison of elements' positions among baseline configuration and designed configurations.

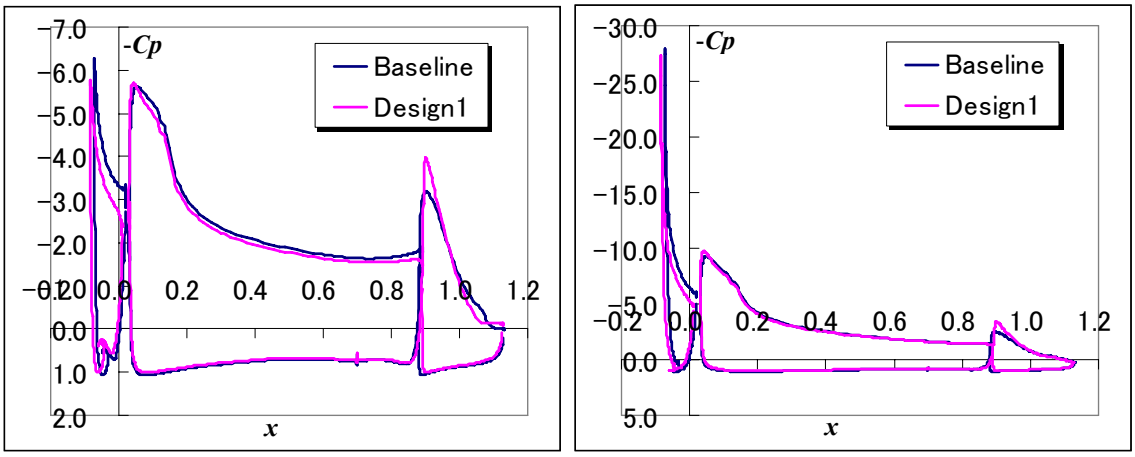

Fig. 12 Comparison of C_p distributions between baseline configuration and design1: (a) AoA=8 degree, (b) AoA=20 degree.

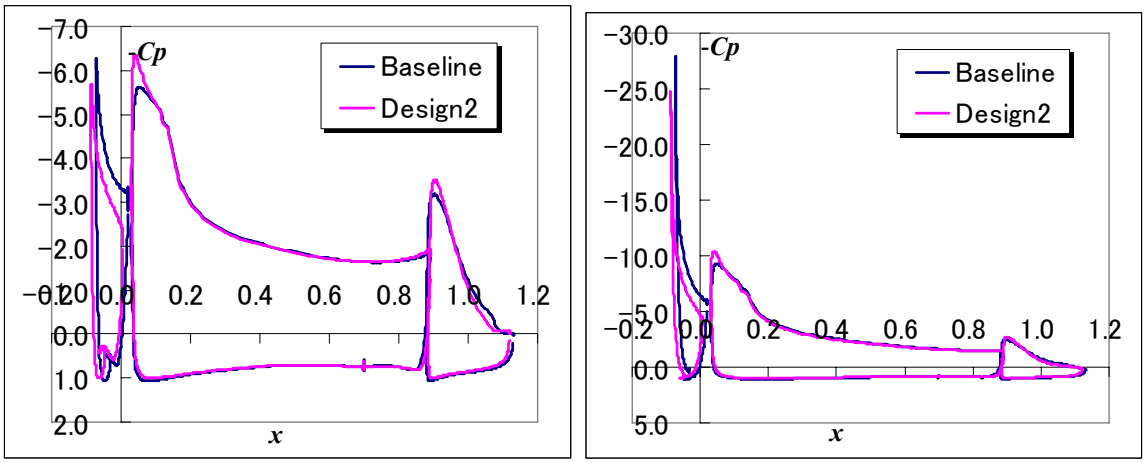

Fig. 13 Comparison of C_p distributions between baseline configuration and design2: (a) AoA=8 degree, (b) AoA=20 degree.

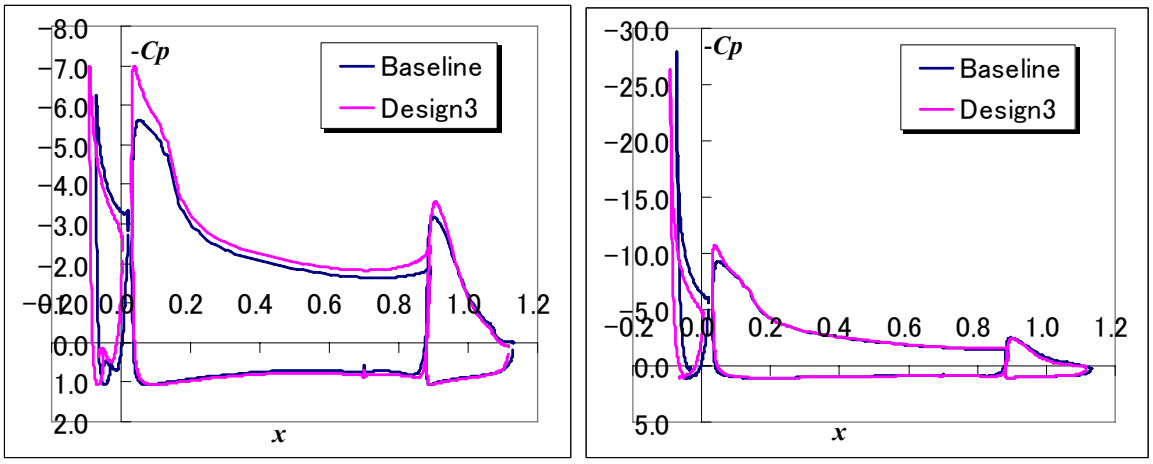

Fig. 14 Comparison of C_p distributions between baseline configuration and design3: (a) AoA=8 degree, (b) AoA=20 degree.

C. Result of ANOVA

Total variances of models were decomposed into the variance due to each design variable. The proportion to the total variable of design variables and their interactions are shown in Fig. 15. According to Fig. 15(a), the flap setting gives over 70% effect on the C_{l8}. Moreover, according to this figure, the two-way interaction between $overlap_{\text{flap}}$ and gap_{flap} has a large effect on C_{l8}. This result suggests that $overlap_{\text{flap}}$ and gap_{flap} should be designed with considering their interaction carefully. Besides, θ_{flap} has a relative small effect because the maximum point of C_{l8} existent over the upper bound of θ_{flap} (See Fig. 8(b)). Generally the design space should be adapted in such case, however, the design space was determined based on practical use in this case. Therefore, elements' settings should design in this design space. According to Fig. 15(b), the slat and the flap setting both give effect on the C_{l20}. This result suggests that the proper setting of elements for C_{l20} is more difficult than that for C_{l8}. According to this figure, the gap of flap is also important design variable for each objective. Generally, a slat is set to increase stall angle, however, this result suggest that the flap setting has also important to the aerodynamic performance near stall condition. Not only slat but also flap should be designed carefully for near stall condition.

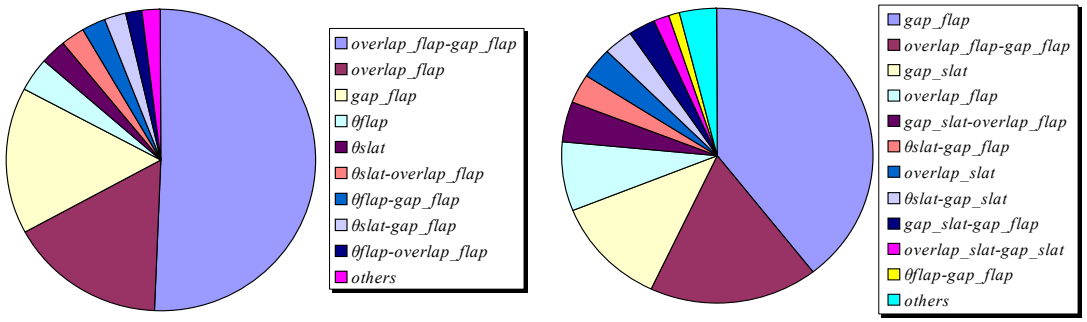

(a) **(b)**

Fig. 15 Total proportion to the total variance of models: (a) C_{l8}, (b) C_{l20}.

IV. Conclusion

Multi-objective design for the elements' settings of the high-lift airfoil consisted of a slat, a main wing, and a flap was performed based on MOGA exploration on the kriging models. The models were used to reduce computational cost. There were two objective functions: maximizing lift coefficient at a landing condition (C_{l8}), maximizing lift coefficient near stall condition (C_{l20}). Flowfields were simulated by solving the Navier-Stocks

equations with Spalart-Allmaras turbulent model using the multi-block structured grid method. The computational grids were deformed automatically for each design.

In this study, the objective functions, C_{l8} and C_{l20}, were transformed to the corresponding EI values on the kriging model and global optimization was performed based on maximizing their values. Using kriging surrogate model, the computational cost can be reduced and EI value permit to carry out high efficient design on the kriging model. To explore the maximum EI values, DRMOGA, a modified version of MOGA, was utilized. The resulting designs were also used as the additional samples to update the kriging models.

Through the present method, the solutions based on the EI maximization advanced to the optimum direction in the solution space. As the result, element settings that give higher performance than that of baseline were successfully obtained. This result suggests that the present method using the kriging based MOGA can be applied to the multi-objective problem while reducing computational time drastically.

In order to obtain the information about design space, ANOVA which is one of the data mining techniques is applied to the sampling result. This result shows the useful information for the design.

References

[1] van Dam, C. P., "The aerodynamic design of multi-element high-lift systems for transport airplanes," *Progress in Aerospace Science*, Vol. 38, 2002, pp. 101-144.

[2] Smith, A. M. O.,"High-Lift Aerodynamics, Journal of Aircraft," Vol. 12, No. 6, 1975, pp. 501-530.

[3]Murayama, M., Lei, Z., Mukai, J., and Yamamoto, K.,"CFD Validation for High Lift Devices: Three-Element Airfoil," *Proceedings of 2004 KSAS-JSASS Joint Symposium on Aerospace Engineering* , 2004.

[4]Mani, M., and Bushm R. H.,: Overlapping Grid Method for High-Lift and Store Carriage Applications, AIAA Paper 93-3428, 1993.

[5]Mathias, D. L., and Cummings, R. M., "Navier-Stokes Analysis of the Flow About a Flap Edge," *Journal of Aircraft*, Vol. 35, No. 6, 1998, pp. 833-838.

[6]Eyi, S., Lee, K. D., Rogers, S. E., and Kwak, D.,"High-Lift Design Optimization Using Navier-Stokes Equations," Journal of Aircraft, Vol. 33, No. 3, 1996, pp. 499-504.

[7] Jeong, S., Murayama, M., and Yamamoto, K.,"Efficient Optimization Design Method Using Kriging Model," *Journal of Aircraft*, Vol. 42, 2005, pp.413-420.

[8] Donald, R., J., Matthias, S. and William, J. W.,"Efficient Global Optimization of Expensive Black-Box Function," *Journal of global optimization*, Vol. 13, 1998, pp. 455-192.

[9] Hiroyasu, T., Miki, M. and Watanabe, S., "The New Model of Parallel Genetic Algorithm in Multi-Objective Optimization Problems (Divided Range Multi-Objective Genetic Algorithm)," *IEEE Proceedings of the Congress on Evolutionary Computation 2000*, Vol. 1, 2000, pp. 333-340.

[10]Kanazaki, M., Obayashi, S., and Nakahashi, K.,"Exhaust Manifold Design with Tapered Pipes Using Divided Range MOGA," *Engineering Optimization*, Vol. 36, Number 2, 2004, pp. 149-164.

[11]Sack, J., Welch, W. J., Mitchell, T. J., and Wynn, H. P., "Design and Analysis of Computer Experiments (with Discussion)," Statistical Science, Vol. 4, 1989, pp. 409-435.

[12] Takaki, R., Yamamoto, K., Yamane, T., Enomoto, S. and Mukai, J.,"The Development of the UPACS CFD Environment," *High Performance Computing*, *Proceedings of ISHPC 2003*, *Springer*, 2003, pp. 307-319.

[13] Crumpton, P. I. and Giles, M. B.,"Implicit time accurate solutions on unstructured dynamic grids," AIAA Paper 95-1671-CP, 1995, pp. 284-294.

[14] Mckay, M. D., Beckman, R. J. and Conover, W. J., "A Comparison of Three Methods for Selecting Values of Input Variables in the Analysis of Output from a Computer Code," *Technometric*, Vol. 21, No. 2, 1979, pp. 239-245.